CHEMISTRY & CHEMICAL TECHNOLOGY

Chem. Chem. Technol., 2023,
Vol. 17, No. 3, pp. 503–509

Chemistry

PHOTOCATALYTIC DEGRADATION OF POLYETHYLENE PLASTICS USING $MgAl_2O_4$ NANOPARTICLES PREPARED BY SOLID STATE METHOD

Sajda .S. Affat[1, ✉], *Saad Shahad Mohammed*[1]

https://doi.org/10.23939/chcht17.03.503

Abstract. In this study, $MgAl_2O_4$ nanoparticles with different calcination times were synthesized for photocatalytic applications. Different analyses techniques such as XRD, SEM, EDX, UV-visible, and FTIR were performed to investigate the structural, chemical, optical, and morphological properties of the synthesized nanoparticles. XRD analysis revealed the formation $MgAl_2O_4$ spinel structure. UV-Visible measurements indicate that $MgAl_2O_4$-2 nanoparticles had a narrower energy gap compared to $MgAl_2O_4$-1 and $MgAl_2O_4$-3. Results of SEM analysis revealed that the synthesized $MgAl_2O_4$ nanoparticles consist of small aggregated particles with (40-60 nm) particles size. EDX measurements confirmed the formation of $MgAl_2O_4$ nanoparticles without any impurities. The photocatalytic performance was evaluated by the photodegradation of polyethylene plastics using $MgAl_2O_4$ nanoparticles under UV irradiation. The FT-IR measurements before and after the degradation of polyethylene plastics confirm the formation of new functional groups as a result of photodegradation processes.

Keywords: nanoparticles, polyethylene, XRD, $MgAl_2O_4$, degradation.

1. Introduction

The annual manufacture of plastic products has exponentially grown over the past decades, with about (370 million tons) being produced in 2019.[1] Plastics are inexpensive, durable, and lightweight materials, which make them appropriate for numerous consumer products in everyday life.[2,3] However, accumulation of the plastic wastes in the environment has been of large concern causing long-term economical, environmental, and management of pollution problems.[4] Polyethylene plastics are frequently used in agriculture such as mulching, greenhouse, and tunnel film. For example, mulching film especially has contributed to enhancing farming techniques. This film has the efficiency for maintaining soil heat and moisture and preventing the propagation of weeds and vermin. As the microorganisms are unable to degrade the artificial plastics,[5] waste plastics ignored in nature persist sometimes for many centuries and cause public concern.[6] Sunlight irradiation represents one of the important environmental factors that initiate the transformation of pollutants, thus posing a great significance in the bioeffect of contaminants and environmental behavior.[7] A few studies indicated that solar light triggering the photodegradation of plastic materials, possibly leading to structural defects,[8] surface oxidation,[9] generation of persistent free radicals[10] and nanoparticles.[11] Compared with many studies concerned with the photodegradation of environmental pollutants,[12,13] few studies were performed on the degradation of plastics, for instance, polyethylene plastics biologic-photocatalytic degradation by Zalerion maritimum[14] and nanomaterials like N-doped TiO_2,[15-19] titania nanotubes,[20] Pt/ZnO,[21] ZnO.[22] In this paper, $MgAl_2O_4$ nanoparticles were synthesized *via* solid-state method and were used as catalysts for the photodegradation of polyethylene plastics under UV irradiation.

2. Experimental

2.1. Chemicals

Analytical grade aluminium nitrate, magnesium sulfate and dimethyl sulfoxide obtained from Sigma Aldrich were used without further purification. Polyethylene plastics used in photocatalytic tests were purchased from a local market.

2.2. Preparation of $MgAl_2O_4$ Nanoparticles

Magnesium aluminates nanoparticles were synthesized *via* solid-state method. 0.5 mmol (0.0601 g) of $MgSO_4$ were mixed and ground carefully in a mortar with 1 mmol (0.375 g) of $Al(NO_3)_3{\cdot}9H_2O$ to obtain a practically homogeneous powder. Then, the obtained mixture was placed into crucible (25 mL) and transferred to an electrical furnace, where it was subjected to thermal treatment at

[1] Department of chemistry, College of Science, University of Thi-Qar
✉ *sajida.j_mschem@sci.utq.edu.iq; saad.sh_chem@sci.utq.edu.iq*

1273 K for 6 h ($MgAl_2O_4$-1), 12 h ($MgAl_2O_4$-2), and 18 h ($MgAl_2O_4$-3). Finally, the crucible containing the mixture was allowed to cool normally until reaching room temperature, and the resulted powder was collected for analyses and photocatalytic tests.

2.3. Photocatalytic Performance

The photocatalytic performance of the prepared powder was evaluated by testing the photocatalytic degradation of polyethylene plastics (PEP). Firstly, the PEP had been cut into small pieces (3 cm × 3 cm) and placed in a Petri dish. An adequate volume (20 mL) of dimethyl sulfoxide (DMSO) was poured into the Petri dish and spread over the PEP to drench it in DMSO. Then, the Petri dish was transferred to a photoreactor. The photodegradation of polyethylene plastics was performed using a photochemical immersion well reactor (400 W medium pressure mercury lamp, light output $5 \cdot 10^{19}$ photons/s) and the PEP was irradiated continuously for five hours. At every one hour, small pieces of PEP were collected and analyzed by FTIR to determine the photodegradation efficiency. Also, the percentage of weight loss of PEP resulting from photodegradation is calculated according to the following equation:

$$\text{Weight loss } \% = \left(\frac{W_i - W_f}{W_f} \right) \cdot 100 \qquad (1)$$

where W_i and W_f are the initial and final weight (after degradation) of PEP, respectively.

2.4. Characterization

The X-ray diffractions patterns of prepared $MgAl_2O_4$ nanoparticles were measured by the XRD 6000 diffractometer instrument (Shimadzu, Japan) using (Cu-Kα) radiation in the range from 20° to 80°. The bonds and the functional groups of all samples were investigated by Fourier transform-infrared spectroscopy (FTIR) (IR affinity-1, Shimadzu, Japan). The morphology and microstructure of the $MgAl_2O_4$ nanoparticle were characterized by a scanning electron microscope (SEM, MIRA3 TESCAN, Hitachi, Japan). The optical properties were measured by UV-absorption spectrum in the range of 200–800 nm using UV-visible spectrophotometer (UV-1800, Shimadzu, Japan).

3. Results and Discussion

3.1. XRD Analysis

Fig. 1 show the obtained XRD patterns of $MgAl_2O_4$-1, $MgAl_2O_4$-2 and $MgAl_2O_4$-3 nanoparticles. The resulted nanoparticles have the $MgAl_2O_4$ spinel structure characteristics peaks (JCPDS card 77-0435) and no peaks of impurities or other compounds are observed. Also, the diffraction peaks intensity increases gradually and the peaks become sharper as the calcination time increases. Table 1 shows the calculated crystallites size (D_p) of the $MgAl_2O_4$ samples treated at different times. It is clearly observed that the crystallites size of all resulted samples are below 50 nm and the samples calcined for 18 h have the larger crystallite size.

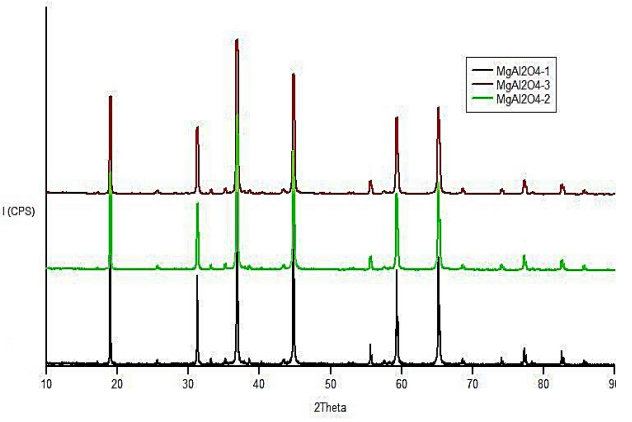

Fig. 1. XRD patterns of $MgAl_2O_4$ nanoparticles

Table1. Calculated crystallites size

Sample	2theta	FWHM	D_p (nm)
$MgAl_2O_4$-1	36.822	0.18609	46.99
$MgAl_2O_4$-2	36.893	0.1832	47.74
$MgAl_2O_4$-3	36.862	0.18121	48.26

3.2. Surface Morphology

$MgAl_2O_4$ nanoparticles surface morphology has been investigated using SEM images (Fig. 2). SEM images revealed that the synthesized $MgAl_2O_4$ consists of small aggregated nanoparticles with 40-60 nm particles size.

3.3. EDX Analysis

The elemental composition of $MgAl_2O_4$ samples were detected by EDX analysis (Fig. 3). EDX measurements show that the synthesized nanoparticles mainly consist of aluminum, magnesium, and oxygen without any impurities.

3.4. FT-IR Analysis

Fig. 4 shows the FTIR spectra of $MgAl_2O_4$ treated at different calcination times. From the spectra, we can observe that the characteristic vibrations of the Mg-O and Al-O bonds appear in the region of 500–700 cm^{-1}. Also, it was noted that all spectra contain bands around wavenumber of 3500 cm^{-1} and 1650 cm^{-1} attributed to the vibrations of O-H group stretching and bending, respectively. However, the weak band located at about 2300 cm^{-1} corresponds to the C=O stretch vibration bond of the CO_2 from the air.

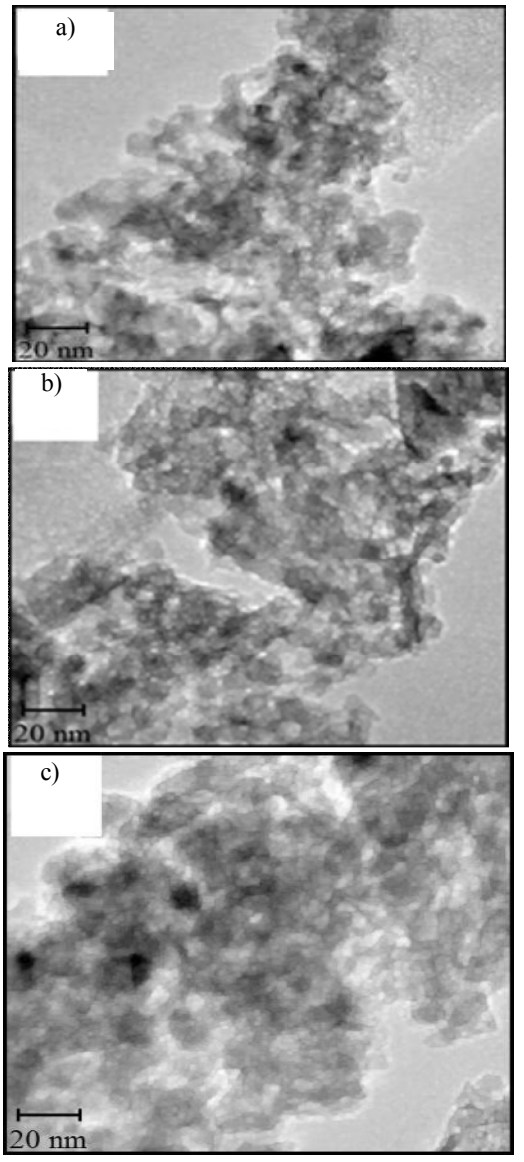

Fig. 2. SEM images (a) $MgAl_2O_4$-1 (b) $MgAl_2O_4$-2 (c) $MgAl_2O_4$-3

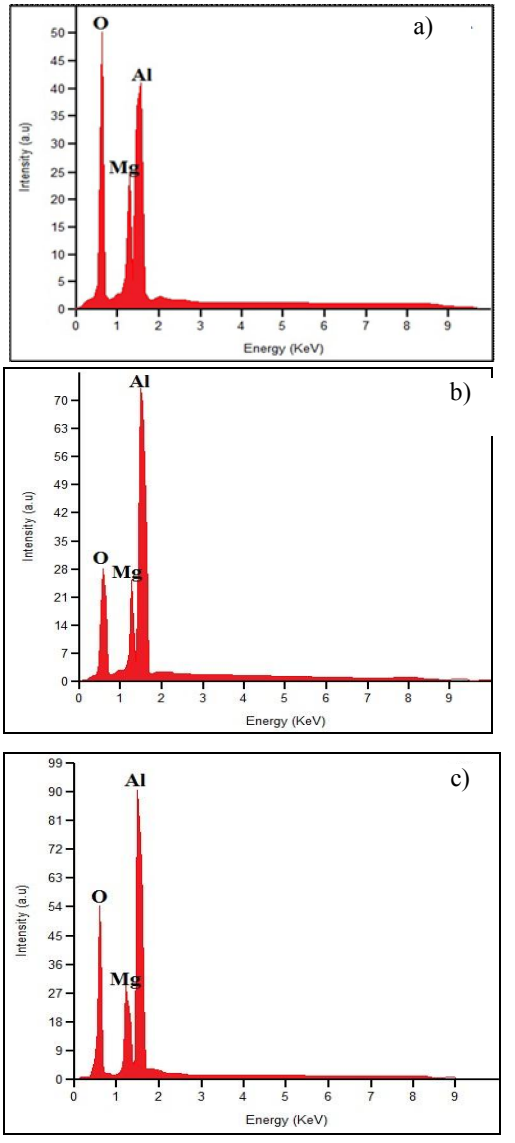

Fig. 3. EDX spectrum (a) $MgAl_2O_4$-1 (b) $MgAl_2O_4$-2 (c) $MgAl_2O_4$-3

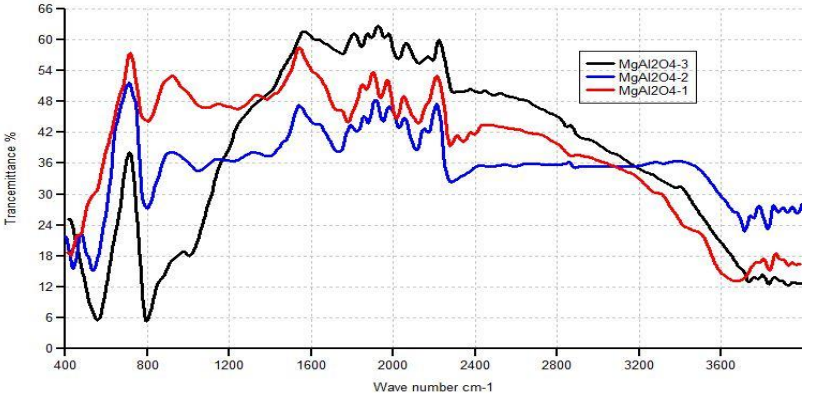

Fig. 4. FT-IR spectra $MgAl_2O_4$-1, $MgAl_2O_4$-2, $MgAl_2O_4$-3

3.5. UV-Visible Analysis

The optical properties extracted from UV-visible spectra of $MgAl_2O_4$ nanoarticles are shown in Fig. 5 and the corresponded energy gap calculated from Tauc relation plotted in Fig. 6. UV-visible absorption measurements indicates that the maximum absorption of synthesized $MgAl_2O_4$ nanoparticles were at 486, 435, and 420 nm for $MgAl_2O_4$-1, $MgAl_2O_4$-2, and $MgAl_2O_4$-3 respectively. Also, the calculated energy gap were 3.55, 2.85, and 2.95 eV for $MgAl_2O_4$ -1, $MgAl_2O_4$ -2, and $MgAl_2O_4$ -3 respectively.

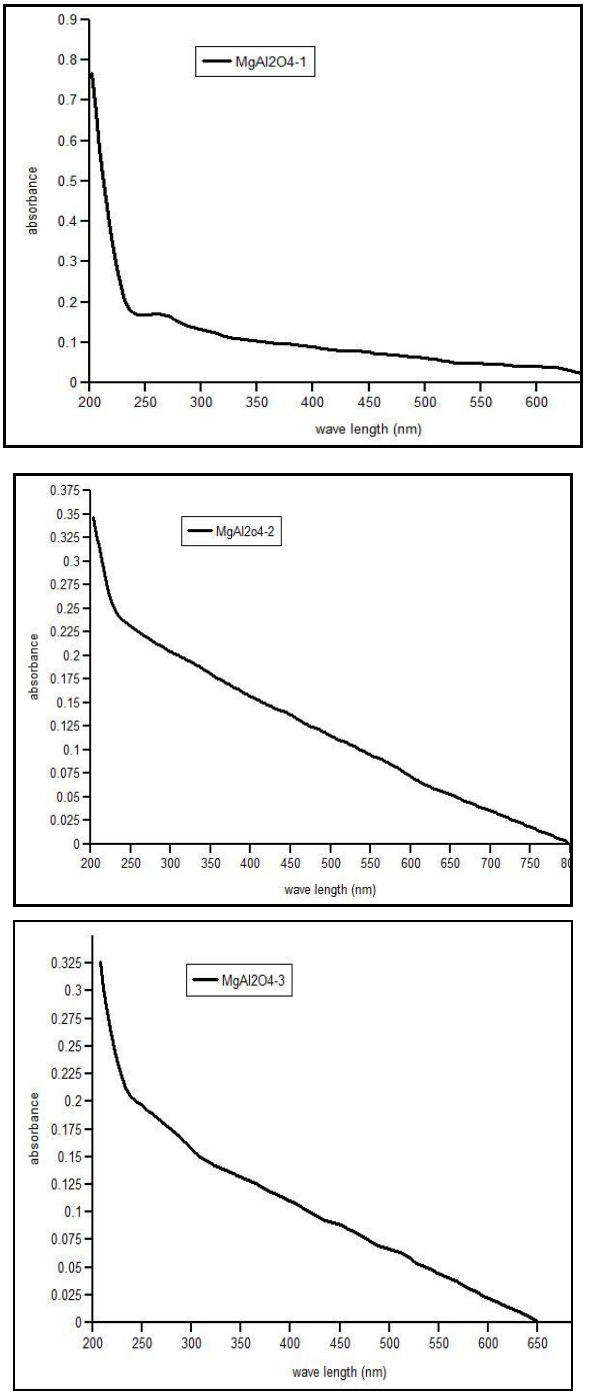

Fig. 5. UV-Visible spectra of synthesized $MgAl_2O_4$ nanooparticles

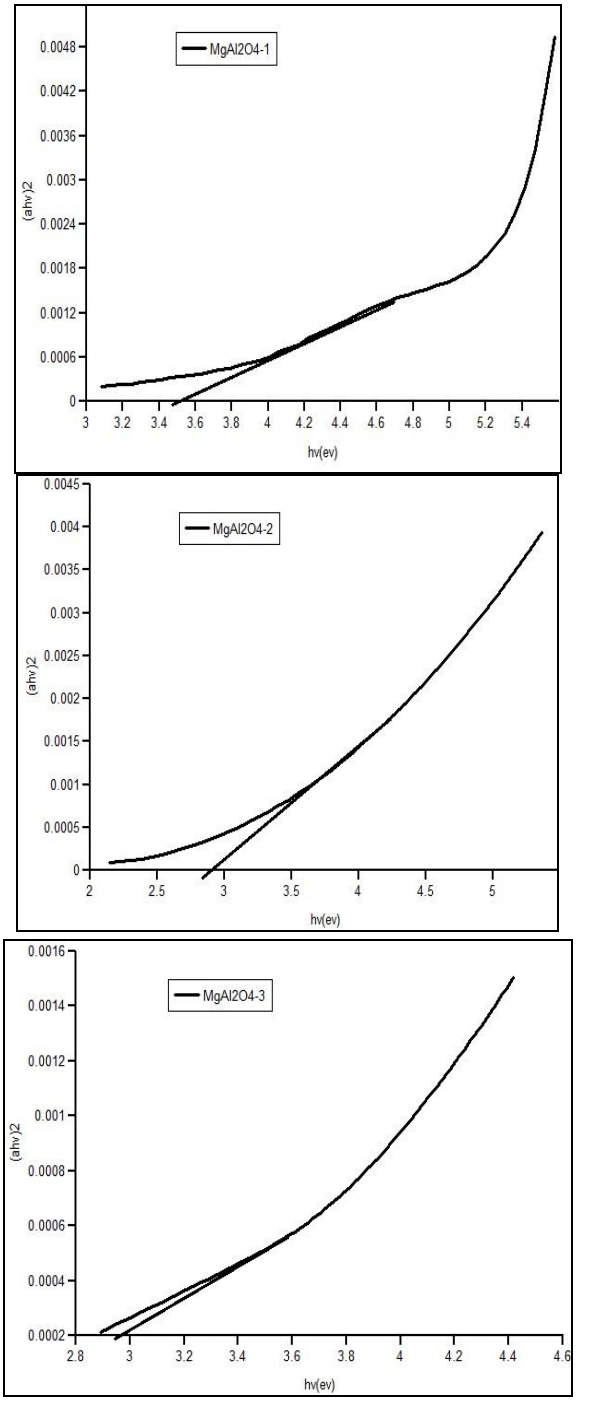

Fig. 6. Tauc plot of synthesized $MgAl_2O_4$ nanooparticles

3.6. Polyethylene Plastics Photocatalytic Degradation

3.6.1. Weight Loss

Fig. 7 shows the weight loss of polyethylene plastics induced by UV irradiation, $MgAl_2O_4$ and UV-$MgAl_2O_4$ with different samples for 5 h. No detectable weight loss was recorded for the photodegradation of polyethylene plastics under UV irradiation. On the contrary, noticeable weight loss has been recorded for the polyethylene plastics using $MgAl_2O_4$ under UV irradiation. Moreover, the weight loss percentage for polyethylene plastics varied with different $MgAl_2O_4$ samples. The irradiation of polyethylene plastics in the presence of $MgAl_2O_4$-2 nanoparticles showed the highest degradation rate (82 %), while the lowest weight loss (60 %) was recorded in the presence of $MgAl_2O_4$-2 nanoparticles.

3.6.2. Chemical Properties of Polyethylene Plastics

FT-IR analysis for polyethylene plastics was carried out to investigate the difference in the chemical properties before and after photodegradation. Fig. 8 shows the FT-IR spectrum of polyethylene plastics before degradation and after photodegradation with $MgAl_2O_4$-1, $MgAl_2O_4$-2, and $MgAl_2O_4$-3 nanoparticles for 5 h. During the photodegradation process, several chemical transformations occur in polyethylene plastics and several new groups are observed such as peroxide, carbonyl, hyperoxide, and unsaturated bonds. As can be seen in Fig. 8, the new peaks within the range of 1700–1800 cm^{-1} refer to the formation of carbonyl groups, which can be related to ketones, carboxylic acid, esters, and aldehydes. Also, new peaks have been observed in the ranges of 900–940 cm^{-1}, 3600–3650 cm^{-1}, and 1000–1350 cm^{-1}, which can be attributed to vinylidene or vinyl, hydroperoxides or alcohols, and peroxides groups, respectively.

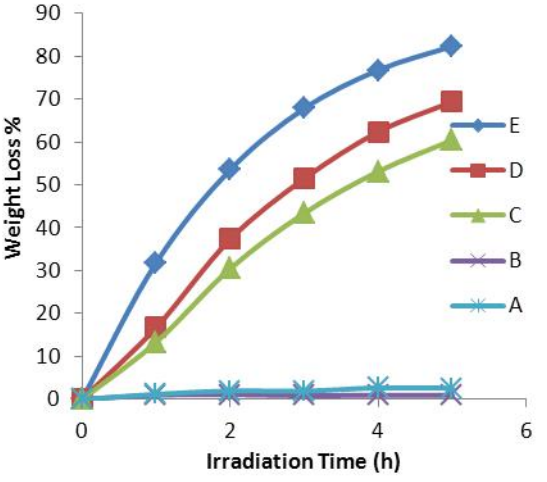

Fig. 7. Polyethylene weight loss (A) under only UV irradiation (B) in the absence of UV irradiation (C-D) in the presence UV irradiation and $MgAl_2O_4$-1, $MgAl_2O_4$-3 and $MgAl_2O_4$-2 respectively

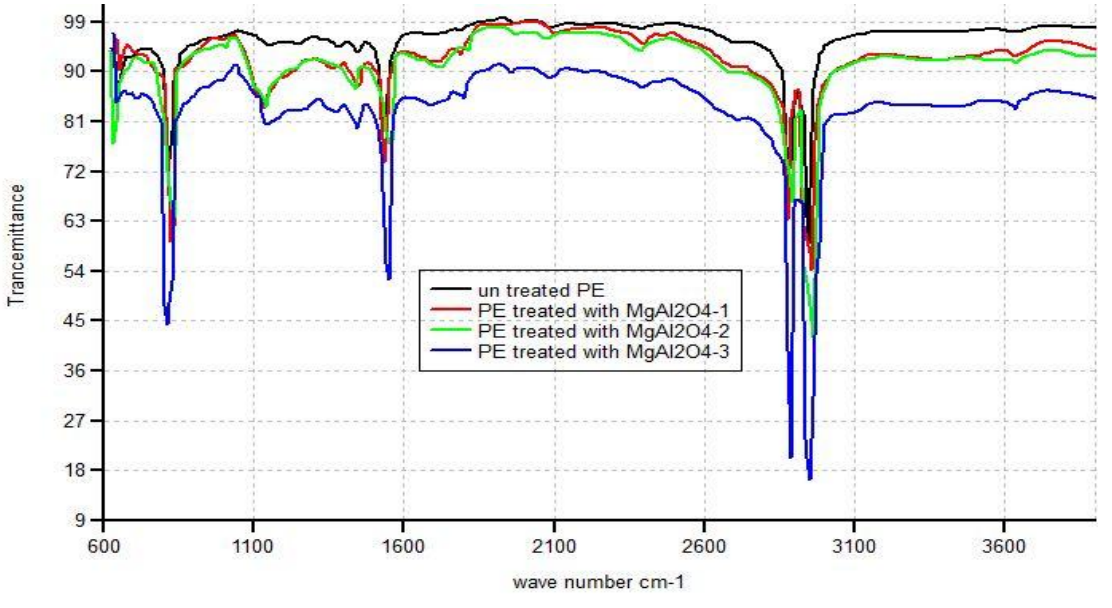

Fig. 8. FT-IR spectra of pure and treated polyethylene plastics

3.6.3. Carbonyl Index

Carbonyl index (CI) can be used to further investigate the formation of carbonyl and hydroxyl groups during the photodegradation of polyethylene plastics. Carbonyl index is used to examine the degree of oxidation of polyethylene plastics and calculated from FT-IR spectra according to the following equation:

$$\textbf{Carbonyl index (CI)} = \frac{abeobance\ cabonyl\ band}{absorbance\ reference\ band}. \quad \ldots(2)$$

The calculated CI values and the corresponded percentage are listed in Table 2.

Table 2. Calculated carbonyl index (CI) of polyethylene plastics

Sample	Carbonyl index	Percentage %
Untreated Polyethylene	2.55	0
Polyethylene- $MgAl_2O_4$-1	3.17	19
Polyethylene- $MgAl_2O_4$-2	3.63	25
Polyethylene- $MgAl_2O_4$-3	3.96	29

The results show that the treatment of polyethylene plastics with $MgAl_2O_4$ under UV irradiation led to the increase in carbonyl index compared with pure polyethylene plastics due to the formation of alcohols and carboxylic acid during the photodegradation process. Also, the carbonyl index for polyethylene treated with $MgAl_2O_4$-3 is larger compared to the polyethylene treated with $MgAl_2O_4$-2 and $MgAl_2O_4$-1, which means the oxidation degree under $MgAl_2O_4$-3 is larger than the others.

3.6.4. Mechanism of Polyethylene Photodegradation

According to advanced oxidation processes (AOPs), the main reactive species are hydroxy ($^{\bullet}OH$) and superoxide ($^{\bullet}O_2^-$) radicals. During photocatalysis, photons (hv) generated from light sources excite the electrons in the valence band of $MgAl_2O_4$. These excited electrons lift up into the vacant conduction band, leaving holes in the valence band, which creates an oxidizing environment, where these holes take part in the degradation process of polyethylene. Under this condition, $MgAl_2O_4$ (h+) accepts electrons from the water producing hydroxyl radical ($^{\bullet}OH$) and hydrogen ion (H^+). Under reducing conditions, electrons in the conduction band produce superoxide ($^{\bullet}O_2$) anion in the presence of air or dissolved oxygen. The degradation of PE depends on the number of holes generated by photons. The generated radicals initiated the degradation process followed by chain breaking, branching, crosslinking, and oxidation of polyethylene. The degradation mechanism of polyethylene has been schematic.

At the onset of the photodegradation process, alkyl chains, in direct contact with the $MgAl_2O_4$ catalyst, are attacked by the radicals. Alkyl radicals are formed by the abstraction of hydrogen inducing breakage of the polymer chain by forming hydroperoxides in the presence of oxygen. Once alkoxy radicals are formed, they propagate within the polymer chain, leading to chain cleavage in the presence of oxygen and generating carbonyl and unsaturated groups. Alkoxy radicals are the main intermediate species that produce aldehydes, ester, ketones, and carboxylic acids in the photooxidation process of polyethylene in the presence of $MgAl_2O_4$ catalyst. Ketone is the key compound in saturated hydrocarbon, which goes through further irradiation and results in the formation of radials and vinyl groups.[20,23] The reactions that are involved in the photolysis or hemolysis of unsymmetrical ketones to form two radicals by α-cleavage of carbon and hydrogen abstraction are called Norrish type I reactions. These radicals can turn into carbon mono-oxides.[24] Ketones may form chain end ketone and unsaturated groups (vinyl and vinylidene) through abstraction of γ hydrogen from long polymeric ketones, the reaction is well known as Norrish type II. These carbonyl groups can be further oxidized to form volatile organic compounds like ethane, formaldehyde, *etc*.,[25] and can mineralize to CO_2 and H_2O.

4. Conclusions

This study investigated the photodegradation of polyethylene plastics using the synthesized $MgAl_2O_4$ nanoparticles. $MgAl_2O_4$ catalyst samples were successfully prepared by the solid-state method and characterized by SEM, UV-Visible, XRD, EDX and FTIR techniques. The characterization results confirmed the formation of a pure $MgAl_2O_4$ structure with 40–60 nm particles size and 3.55–2.85 eV energy gap. The photodegradation results demonstrated that the $MgAl_2O_4$ catalyst promotes the degradation of polyethylene plastics under UV irradiation. Furthermore, the photodegradation results confirmed that the polyethylene plastics weight loss and carbonyl index are higher when plastics are irradiated in the presence of $MgAl_2O_4$-2 compared with $MgAl_2O_4$-3 and $MgAl_2O_4$-1 nanoparticles.

References

[1] Plastics Europe, 2020. Plastics – the Facts 2020: An Analysis of European Plastics Production, Demand and Waste Data Brussels, Belgium.

[2] Thompson, R.C.; Swan, S.H.; Moore, C.J.; vom Saal, F.S. Our Plastic Age. *Phil. Trans. R. Soc. B* **2009**, *364*, 1973-1976. https://doi.org/10.1098/rstb.2009.0054

[3] Wang, J.; Tan, Z.; Peng, J.; Qiu, Q.; Li, M. The Behaviors of Microplastics in the Marine Environment. *Mar. Environ. Res*. **2016**, *113*, 7-17. https://doi.org/10.1016/j.marenvres.2015.10.014

[4] Singh, B.; Sharma, N. Mechanistic Implications of Plastic Degradation. *Polym. Degrad. Stab*. **2008**, *93*, 561-584. https://doi.org/10.1016/j.polymdegradstab.2007.11.008
[5] Mueller, R.-J. Biological Degradation of Synthetic Polyesters—Enzymes as Potential Catalysts for Polyester Recycling. *Process Biochem*. **2006**, *41*, 2124-2128. https://doi.org/10.1016/j.procbio.2006.05.018
[6] Shimao, M. Biodegradation of Plastics. *Curr. Opin. Biotechnol*. **2001**, *12*, 242-247. https://doi.org/10.1016/S0958-1669(00)00206-8
[7] Miranda-García, N.; Suárez, S.; Sánchez, B.; Coronado, M.; Malato, S.; Maldonado, I. Photocatalytic Degradation of Emerging Contaminants in Municipal Wastewater Treatment Plant Effluents Using Immobilized TiO_2 in a Solar Pilot Plant. *Appl. Catal. B* **2011**, *103*, 294-301. https://doi.org/10.1016/j.apcatb.2011.01.030
[8] Song, Y.K.; Hong, S.H.; Jang, M.; Han, G.M.; Jung, S.W.; Shim, W.J. Combined Effects of UV Exposure Duration and Mechanical Abrasion on Microplastic Fragmentation by Polymer Type. *Environ. Sci. Technol*. **2017**, *51*, 4368-4376. https://doi.org/10.1021/acs.est.6b06155
[9] Hämer, J.; Gutow, L.; Köhler, A.; Saborowski, R. Fate of Microplastics in the Marine Isopod *Idotea emarginata*. *Environ. Sci. Technol*. **2014**, *48*, 13451-13458. https://doi.org/10.1021/es501385y
[10] Zhu, K.; Jia, H.; Zhao, S.; Xia, T.; Guo, X.; Wang, T.; Zhu, L. Formation of Environmentally Persistent Free Radicals on Microplastics under Light Irradiation. *Environ. Sci. Technol*. **2019**, *53*, 8177-8186. https://doi.org/10.1021/acs.est.9b01474
[11] Gigault, J.; Pedrono, B.; Maxit, B.; Ter Halle, A. Marine Plastic Litter: The Unanalyzed Nano-Fraction. *Environ. Sci. Nano* **2016**, *3*, 346-350. https://doi.org/10.1039/C6EN00008H
[12] AL-Zamili, F.; Abass, A.; Najim, A. Effect of Some Organic Fillers on the Mechanical Properties of High Density Polyethylene. *J.Thi-Qar Sci*. **2009**, *1*, 27-34.
[13] Hammed, M.; Hamad, T. Study Of TiO_2 Nanoparticles Induction for Biological System. *Thi-Qar Medical Journal* **2019**, *17*, 110-117.
[14] Paço, A.; Duarte, K.; da Costa, J.P.; Santos, P.S.M.; Pereira, R.; Pereira,M.E.; Freitas, A.C.; Duarte, A.C.; Rocha-Santos, T.A.P. Biodegradation of Polyethylene Microplastics by the Marine Fungus Zalerion Maritimum. *Sci. Total Environ*. **2017**, *586*, 10-15. https://doi.org/10.1016/j.scitotenv.2017.02.017
[15] Ariza-Tarazona, M.C.; Villarreal-Chiu, J.F.; Hernández-López, J.M.; de la Rosa, J.R.; Barbieri, V.; Siligardi, C.; Cedillo-González, E.I. Microplastic Pollution Reduction by a Carbon and Nitrogen-Doped TiO_2: Effect of pH and Temperature in the Photocatalytic Degradation Process. *J. Hazard. Mater*. **2020**, *395*, 122632. https://doi.org/10.1016/j.jhazmat.2020.122632
[16] Ariza-Tarazona, M.C.; Villarreal-Chiu, J.F.; Barbieri, V.; Siligardi, C.; Cedillo-González, E.I. New Strategy for Microplastic Degradation: Green Photocatalysis Using a Protein-Based Porous N-TiO_2 Semiconductor. *Ceram. Int*. **2019**, *45*, 9618-9624. https://doi.org/10.1016/j.ceramint.2018.10.208
[17] Kulkarni, M.; Thakur, P. The Effect of UV/TiO_2/H_2O_2 Process and Influence of Operational Parameters on Photocatalytic Degradation of Azo Dye in Aqueous TiO_2 Suspension. *Chem. Chem. Technol*. **2010**, *4*, 265-270. https://doi.org/10.23939/chcht04.04.265
[18] Nikolenko, A.; Melnykov, B. Photocatalytic Oxidation of Formaldehyde Vapour Using Amorphous Titanium Dioxide. *Chem. Chem. Technol*. **2010**, *4*, 311-315. https://doi.org/10.23939/chcht04.04.311
[19] Coronel, S.; Pauker, Ch.S.; Jentzsch, P.V.; de la Torre, E.; Endara, D.; Muñoz-Bisesti, F. Titanium Dioxide/Copper/Carbon Composites for the Photocatalytic Degradation of Phenol. *Chem. Chem. Technol*. **2020**, *14*, 161-168. https://doi.org/10.23939/chcht14.02.161
[20] Ali, S.S.; Qazi, I.A.; Arshad, M.; Khan, Z.; Voice, T.C.; Mehmood, Ch.T. Photocatalytic Degradation of Low Density Polyethylene (LDPE) Films Using Titania Nanotubes. *Environ. Nanotechnol. Monit. Manag*. **2016**, *5*, 44-53. https://doi.org/10.1016/j.enmm.2016.01.001
[21] Tofa, T.S.; Ye, F.; Kunjali, K.L.; Dutta, J. Enhanced Visible Light Photodegradation of Microplastic Fragments with Plasmonic Platinum/Zinc Oxide Nanorod Photocatalysts. *Catalysts* **2019**, *9*, 819. https://doi.org/10.3390/catal9100819
[22] Tofa, T.S.; Kunjali, K.L.; Paul, S.; Dutta, J. Visible Light Photocatalytic Degradation of Microplastic Residues with Zinc Oxide Nanorods. *Environ Chem Lett* **2019**, *17*, 1341-1346. https://doi.org/10.1007/s10311-019-00859-z
[23] Gardette, M.; Perthue, A.; Gardette, J.-L.; Janecska, T.; Földes, E.; Pukánszky, B.; Therias, S. Photo- and Thermal-Oxidation of Polyethylene: Comparison of Mechanisms and Influence of Unsaturation Content. *Polym. Degrad. Stab*. **2013**, *98*, 2383-2390. https://doi.org/10.1016/j.polymdegradstab.2013.07.017
[24] Dinda, B. *Essentials of pericyclic and photochemical reactions*. Vol. 93; Springer: Switzerland, 2017.
[25] Shang, J.; Chai, M.; Zhu, Y. Photocatalytic Degradation of Polystyrene Plastic under Fluorescent Light. *Environ. Sci. Technol*. **2003**, *37*, 4494-4499. https://doi.org/10.1021/es0209464

Received: November 09, 2021 / Revised: December 21, 2021 / Accepted: April 16, 2022

ФОТОКАТАЛІТИЧНА ДЕГРАДАЦІЯ ПОЛІЕТИЛЕНОВИХ ПЛАСТИКІВ ЗА ДОПОМОГОЮ НАНОЧАСТИНОК $MgAl_2O_4$, СИНТЕЗОВАНИХ ТВЕРДОФАЗНИМ МЕТОДОМ

Анотація. *У цій роботі було синтезовано наночастинки $MgAl_2O_4$ з різним часом прожарювання для фотокаталітичних застосувань. Для дослідження структурних, хімічних, оптичних і морфологічних властивостей синтезованих наночастинок було використано різні методи аналізу, такі як XRD, SEM, EDX, УФ-видима та FTIR спектроскопія. XRD аналіз показав утворення структури шпінелі $MgAl_2O_4$. Вимірювання в УФ-видимому діапазоні вказують, що наночастинки $MgAl_2O_4$-2 мають вужчу енергетичну щілину порівняно з $MgAl_2O_4$-1 і $MgAl_2O_4$-3. Результати SEM-аналізу показали, що синтезовані наночастинки $MgAl_2O_4$ складаються з дрібних агрегованих частинок розміром 40-60 нм. EDX вимірювання підтвердили утворення наночастинок $MgAl_2O_4$ без будь-яких домішок. Фотокаталітичну ефективність оцінювали через фотодеградацію поліетиленових пластиків за допомогою наночастинок $MgAl_2O_4$ під УФ-опроміненням. FTIR вимірювання до та після деградації поліетиленових пластмас підтверджують утворення нових функціональних груп у результаті процесів фотодеградації.*

Ключові слова: *наночастинки, поліетилен, XRD, $MgAl_2O_4$, деградація.*